



CHORUS

This is the accepted manuscript made available via CHORUS. The article has been published as:

Thermoelectric Detection of Spin Waves

H. Schultheiss, J. E. Pearson, S. D. Bader, and A. Hoffmann

Phys. Rev. Lett. **109**, 237204 — Published 4 December 2012

DOI: [10.1103/PhysRevLett.109.237204](https://doi.org/10.1103/PhysRevLett.109.237204)

Thermoelectric detection of spin waves

H. Schultheiss,¹ J.E. Pearson,¹ S.D. Bader,^{1,2} and A. Hoffmann¹

¹Materials Science Division, Argonne National Laboratory, Argonne, IL 60439

²Center for Nanoscale Materials, Argonne National Laboratory, Argonne, IL 60439

We report on the thermoelectric detection of spin waves in permalloy stripes via the anomalous Nernst effect. Spin waves are locally excited by a dynamic magnetic field generated from a microwave current flowing in a coplanar waveguide placed on top of a permalloy stripe, which acts as a waveguide for spin waves. Electric contacts at the ends of the permalloy stripe measure a *dc* voltage generated along the stripe. Magnetic field sweeps for different applied microwave frequencies reveal, with remarkable signal-to-noise, an electric voltage signature characteristic of spin-wave excitations. The symmetry of the signal with respect to the applied magnetic field direction indicates that the anomalous Nernst effect is responsible; Seebeck effects, anisotropic magnetoresistance, and voltages due to spin-motive forces are excluded. The dissipation of spin waves causes local heating, that drains into the substrate giving rise to a temperature gradient perpendicular to the sample plane, resulting in the anomalous Nernst voltage.

PACS numbers: 75.40.Gb; 75.40.Mg; 75.75.+a; 85.75.-d

The emerging field of *spin caloritronics* [1] has attracted interest in the research community due to the interactions between spin, charge and heat currents. The research efforts in this field are driven by fundamental questions such as how spin currents are generated from heat currents via the spin Seebeck effect, [2–4] or whether spin currents can transport heat via the spin Peltier effect [5]. Spin waves or magnons are the elementary excitation quanta of a ferromagnet. They play an important role in spin caloritronics since they transport a spin current over mesoscopic distances, even in ferromagnetic insulators, [6] and they can generate thermopower due to magnon drag [7]. However, various effects have to be considered when it comes to electromotive forces generated by magnetization dynamics, especially when temperature gradients are involved. For example, Huang *et al.* [8] identified substrate effects in their spin-dependent thermal transport studies due to anomalous Nernst effects (ANE), and Weiler *et al.* [9] detected a local electric field in a ferromagnetic film generated by ANE when heating the surface with a focused laser; furthermore they used this effect to map the magnetization direction.

In this Letter we demonstrate the generation of an electromotive force due to spin waves via the ANE. The decay of spin waves and the transfer of energy to the phonon system heats the magnetic film. The substrate acts as a heat sink and causes a temperature gradient perpendicular to the surface, which results in an electric field perpendicular to both the temperature gradient and magnetization direction. We show that this approach is suitable for spin wave spectroscopy with no lower wavelength limit and that it enables detection of parametrically excited spin waves in a standard sample geometry. The effect is useful for detecting linear and nonlinear spin waves, and provides another mechanism for voltage generation in spin caloritronic experiments.

The samples under investigation are sputtered Permal-

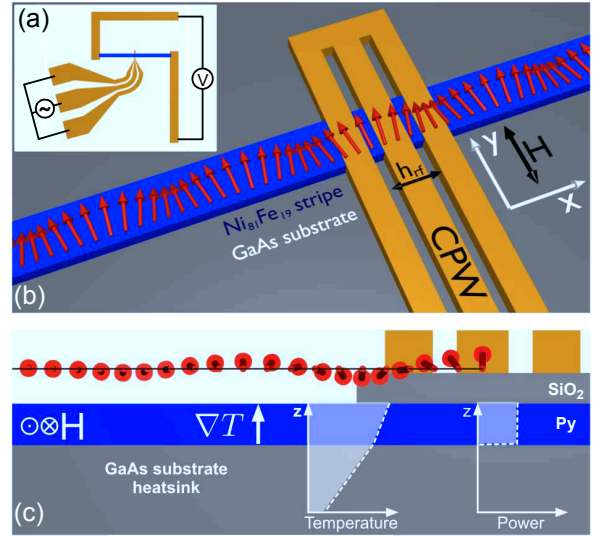


FIG. 1: (color online) (a),(b) Schematic of the sample. The spin wave waveguide (blue) is 2-mm long, 20- μm wide and made from 100-nm thick permalloy on a GaAs substrate. The coplanar waveguide for *rf* excitation and the leads for *dc* voltage measurements are made from 150-nm thick Au. The CPW has a signal-line width of 10 μm and a signal to ground-line separation of 5 μm . (c) Illustration of the *z*-distribution of the dissipated power and resulting temperature profile.

loy (Py, $\text{Ni}_{81}\text{Fe}_{19}$) films with a thickness of 100 nm. These films were patterned on GaAs -substrates into stripes 20- μm wide and 2-mm long using optical lithography and lift-off processes in order to act as waveguides for spin waves. A schematic layout of the sample geometry is shown in Figs. 1. In the middle of the Py stripe we placed the shorted end of a coplanar waveguide (CPW) for spin-wave excitation by microwave currents that generate a dynamic magnetic field \vec{h}_{rf} parallel to the *x*-axis. In the narrow section close to the shorted end the

CPW has a signal line width of $10 \mu\text{m}$ and a signal to ground-line separation of $5 \mu\text{m}$. The CPW is made from sputtered Cr (15 nm) and Au (150 nm) and is electrically isolated from the Py stripe by a 100 nm thick separating layer of sputtered SiO_2 . At the ends of the Py stripe in 1-mm separation from the CPW, are electrical contacts (patterned in the same step as the CPW) for detecting voltages generated along the spin-wave waveguide. The Py stripe is 2-mm long in order to separate the electric contacts and the area of spin-wave excitation. This avoids heating of these contacts and minimizes Seebeck voltages that arise from thermal electromotive forces at the contacts of the Cr/Au leads with the stripe. A static magnetic field \vec{H} is applied in the sample xy -plane. For \vec{H} parallel to the y -axis the torque $\vec{M} \times \vec{h}_{\text{rf}}$ on the magnetization \vec{M} is maximized and allows for efficient excitation of spin waves with frequencies up to 20 GHz that propagate along the x -direction of the Py stripe. The decay length of spin waves in Py for this geometry and these frequencies is of the order of tens of micrometers [10–13]. As a result, the microwave energy transferred from the CPW to the spin waves is dissipated close to the CPW as shown schematically in Fig.1(c). This dissipation results in local heating of the Py stripe, and due to the thermal contact with the GaAs-substrate, which acts as a heat sink, a local temperature gradient ∇T is created in the Py stripe. This gradient perpendicular to the sample plane gives rise to a local electric field due to the anomalous Nernst effect [9]:

$$\vec{E}_{\text{ANE}}(x, y) = -N\mu_0\vec{M}(x, y) \times \nabla T(x, y), \quad (1)$$

where N is the Nernst coefficient and μ_0 is the permeability of free space. This then yields the voltage that builds up between the ends of the spin-wave waveguide (along the x -direction), which is given by:

$$V_{\text{ANE}} = \int \vec{E}_{\text{ANE}}(x, y = 0) \cdot d\vec{x}. \quad (2)$$

Note that due to the cross product in Eq. (1) the electric field $\vec{E}_{\text{ANE}}(x, y)$ is always perpendicular to \vec{M} , therefore, the detected voltage scales with $\cos(\theta)$ where θ is the angle between the applied magnetic field and the y -axis. Hence, the voltages emerging from the ANE are at maximum for \vec{H} applied perpendicular to the Py stripe, which is the starting geometry for the following discussion.

Typical spin-wave spectra that we observe in our sample are shown in Fig. 2 for excitation frequencies ranging from 4 (red) to 20 GHz (purple) in 1 GHz steps while using nominally 5 dBm power. All measurements were performed at room temperature. The microwave amplitudes are modulated with a 1-kHz reference of a lock-in amplifier that is also used for detecting the dc voltage at the end of the Py stripe. Different modulation frequencies ranging from 50 Hz to 20 kHz and a separate measurement without amplitude modulation and

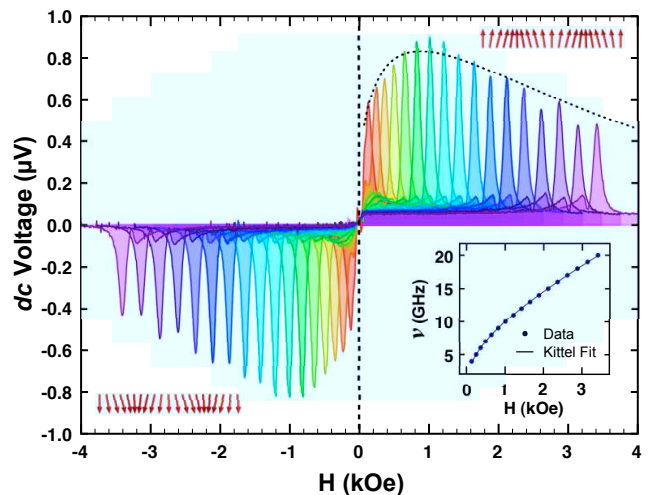


FIG. 2: (color online) Voltage measured between the ends of the permalloy stripe as a function of the magnetic field applied perpendicular to the stripe for frequencies from 4 GHz (red) to 20 GHz (purple) in 1 GHz steps. The dotted line shows a theoretical estimate of the relative power dissipated by the spin waves. The inset shows the peak position vs. applied frequency with a fit to the Kittel equation.

a standard voltmeter resulted in the same voltages and confirmed that the measurements are performed in the steady state. For a given excitation frequency we sweep \vec{H} in the y -direction. The measured voltages show distinct resonance peaks as a function of the magnetic field and change sign upon reversal of the field direction. In the inset of Fig. 2 the excitation frequencies ν are plotted as a function of the resonance field at which the measured voltages have the maximum value. The data points (blue dots) are in excellent agreement with a fit to the Kittel equation [14]:

$$\nu^2 = \left(\frac{\gamma}{2\pi}\right)^2 [H - (N_x - N_y)M_s][H - (N_x - N_z)M_s], \quad (3)$$

where $\gamma = 28 \text{ GHz/T}$ is the gyromagnetic ratio. The fit yields the saturation magnetization $M_s = 905 \text{ kA/m}$ and the dimensionless demagnetizing factors $N_x = 0.001$, $N_y = 0.004$ and $N_z = 0.995$. This fit to the Kittel equation is an approximation since the CPW actually excites not the ferromagnetic resonance (FMR) but spin waves with a finite wavevector. However, the wavevector of the spin waves at the peak maximum is rather small as we show later [see Fig. 4(c)] and the errors for the material parameters mentioned above by fitting using Eq. (3) are negligible. In addition to the position of the resonance peaks, we need to understand the signal strength that first increases as a function of frequency and then decreases for $\nu \geq 10 \text{ GHz}$. The increase of the signal strength for lower frequencies is an indication that the observed effect does not scale with the cone angle of the

magnetization precession: For fixed values of the applied microwave powers, *i.e.* fixed excitation field strength \vec{h}_{rf} , the cone angle of the precession gets smaller for larger frequencies because of the increased value of the static magnetic field at the resonance condition [see Eq. (3)].

Recently, Bakker *et al.* [15] showed that the power dissipation to the lattice originating from the magnetization dynamics increases monotonically with the precession frequency if one assumes that \vec{h}_{rf} is constant. In a real sample, however, there are significant losses of a microwave current flowing in a CPW that get larger for higher frequencies and result in a strong reduction of \vec{h}_{rf} even though the nominal output power of the microwave generator is fixed. The dashed line in Fig. 2 shows the relative power dissipated in the Py stripe calculated following the analysis in [15] and including a frequency dependent power with a loss of 0.34 dB/GHz, which is chosen to match the experimental data and is a reasonable estimate for the losses in our microwave setup consisting of pico-probes and the thin, on-chip CPW. The relative frequency dependence for the dissipated power that causes the local heating and temperature gradient in the Py stripe is in good agreement with the envelope of the measured voltages, which supports the argument for an ANE mechanism.

One alternative that could generate a *dc* voltage in our sample is the rectification of a parasitic microwave current in the Py by an anisotropic magnetoresistance (AMR) [16]. The spin-wave waveguide is capacitively coupled to the CPW in the overlapping area and, hence, we cannot exclude the possibility of a microwave current in the Py stripe. To rule out a possible contribution of AMR we measured the voltage drop over the Py stripe for different in-plane angles of the applied magnetic field, as shown in Fig. 3. For 0° the magnetic field is perpendicular to the Py stripe and the measured voltages are maximum, for $\pm 10^\circ$ and $\pm 20^\circ$ the voltage drops and for 90° the magnetization is parallel to the stripe and the voltage is zero. This is in agreement with an ANE mechanism, as described in Eqs.(1) and (2), but it is in contradiction to the expectation for microwave rectification by AMR, which would scale with $\sin(2\theta)$ [17, 18]. Furthermore, the angular dependence and the sample geometry exclude any signals from anomalous Hall effects [19]. Also, we can exclude contributions from spin-pumping [20] and spin-motive forces, as recently reported by Yamane *et al.* [21], because both contact leads for the voltage detection are at positions where $d\vec{M}/dt = 0$. Any spin-motive forces originating from spin waves traveling to the left and right from the CPW are expected to cancel each other.

Another independent check to verify that the voltage generation is due to ANE is shown in Fig. 3(b). Here we measured the voltage drop over the Py stripe (for H with $\theta = 0^\circ, 180^\circ$) as a function of a *dc* current I_{dc} applied to the CPW. The ohmic heating of the CPW causes a temperature gradient in the Py stripe and, as expected

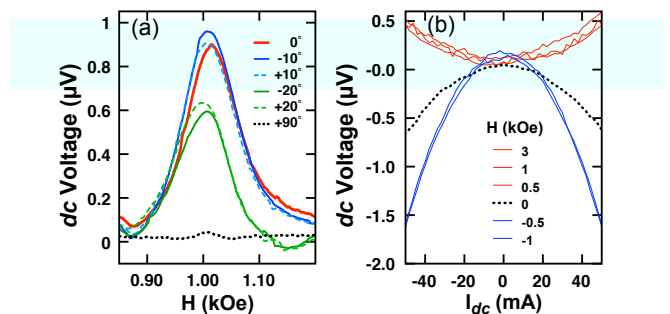


FIG. 3: (color online) (a) Detected voltage for different in-plane angles of the applied magnetic field. For 0° the magnetic field is perpendicular to the Py stripe, for 90° \vec{H} is parallel. (b) Thermoelectric voltage detected while heating the CPW with a *dc* current for different values of the magnetic field applied perpendicular to the Py stripe.

from Eqs. (1) and (2), the measured voltage only depends on the magnitude of the current ($\nabla T \propto I_{dc}^2$) and the direction of \vec{H} but not on its magnitude. The fact that $V(I_{dc})$ is not zero for $\vec{H} = \vec{0}$ is a result of a Seebeck voltage caused by the asymmetric position of the CPW contact leads [see Fig. 1(a)], which causes slightly more heating on the left end of the Py stripe compared to the right end. This Seebeck voltage always adds to the ANE voltage and therefore $|V_{H>0} - V_{H=0}|$ equals $|V_{H<0} - V_{H=0}|$ as can be seen from Fig. 3(b). For the detection of spin-wave resonances this asymmetry and the ohmic heating is negligible for two reasons: First, the microwave power is constant during a field sweep so that a Seebeck voltage due to ohmic heating of the CPW would only cause a constant offset. Second, a microwave power of 5 dBm corresponds to a current of only 8 mA in the CPW, which would result in an offset smaller than 100 nA, as can be seen in Fig. 3(b).

Even though the detection of spin waves by means of ANE does not resolve their wavelength, it has a particular advantage over other techniques, such as inductive detection by antennas [22] or optical methods like magneto optical Kerr effect [23] and Brillouin light scattering [24]: There is practically no lower limit for the spin-wave wavelength λ that can be detected because every spin wave decays and, therefore, causes a temperature gradient. In our measurements this becomes apparent from Fig. 4(a) where we plot the spin-wave resonances at 10 GHz for excitation powers ranging from -9 dBm to 18 dBm in 3 dBm steps. The main resonance peak at 1014 Oe is a direct spin wave excitation with a small wavevector $k = 0.086 \mu\text{m}^{-1}$ ($\lambda = 73 \mu\text{m}$). The values for k and λ result from the crossing point of the 10 GHz excitation line and calculated spin-wave dispersion shown in Fig. 4(c) (upper, red curve). (For details of the dispersion calculations refer to Ref. [11]). To the

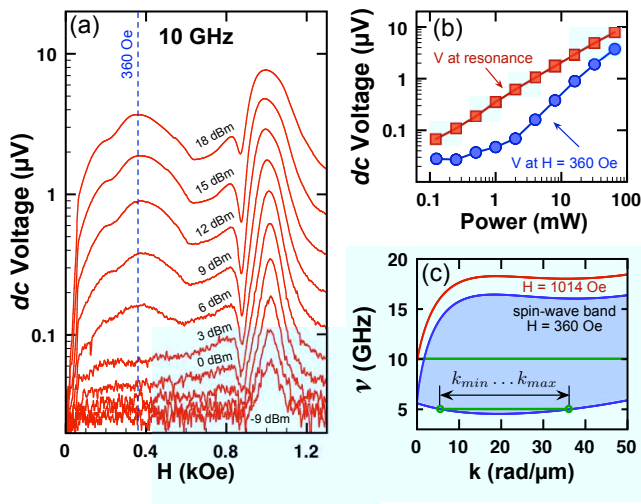


FIG. 4: (color online) (a) Magnetic field sweeps for excitation at 10 GHz for microwave powers ranging from -9 dBm to 18 dBm in 3 dBm steps. (b) Maximum of the detected voltage (red squares) and voltage at a magnetic field of 360 Oe as a function of the applied microwave power. (c) Upper red line: spin-wave dispersion for $H = 1014$ Oe and wavevector perpendicular to \vec{M} , lower blue lines: spin-wave band for $H = 360$ Oe. The green horizontal lines mark the excitation frequency ν and the parametrically excited spin waves at $\nu/2$.

left of the main resonance peak one can see a drop in the measured voltage at 880 Oe. At this field the dispersion gives $k = 0.314 \mu\text{m}^{-1}$ ($\lambda = 20 \mu\text{m}$), which is the wavevector where the excitation efficiency of the 10- μm wide CPW has its minimum [25]. A striking feature visible in Fig. 4(a) is the signature around 360 Oe in the field sweep, which only appears for excitation powers above 6 dBm. At this particular field the crossing point of the spin-wave dispersion and the 10 GHz excitation gives a minimum wavevector of $1.48 \mu\text{m}^{-1}$ ($\lambda = 4.2 \mu\text{m}$) which is too large to be directly excited by the CPW. The only way that spin waves could be excited in this field range with the CPW is via nonlinear, parametric excitation, which means that for a pumping frequency $\nu_{\text{pump}} = 10$ GHz spin waves with 5 GHz are excited. This is also supported by the fact that these spin waves only appear above a threshold power [6 dBm or 4 mW, see Fig.4(b)], which is characteristic for this nonlinear spin-wave excitation [26]. It is also evident from the power dependence of the main resonance peak, which broadens and shifts to lower magnetic fields, that the magnetization is driven into the nonlinear regime. The spin-wave eigenmodes that can be parametrically excited with a pumping frequency of 10 GHz are all the states within the blue spin-wave band at 5 GHz [see Fig.4(c), lower, green line] that cover wavevectors from $k_{\text{min}} = 7.5 \mu\text{m}^{-1}$ to $k_{\text{max}} = 36 \mu\text{m}^{-1}$. These wavevectors correspond to wavelengths from $\lambda_{\text{max}} = 840$ nm to $\lambda_{\text{min}} = 174$ nm.

Note that this is not the minimum wavelength detected in our experiment. For even lower magnetic fields the spin-wave band shifts to lower frequencies and, hence, the maximum wavevector for parametric excitation increases. For example, at a magnetic field of 100 Oe the smallest detected spin-wave wavelength is only 125 nm.

For the parametrically excited spin waves, the short wavelengths and the small group velocity result in a confinement mainly below the CPW, which allows to estimate ∇T : For 6 dBm the spin waves detected at 360 Oe are excited only below the signal line of the CPW and not below the ground lines, because each ground line carries only half the power (3 dBm), which is below the threshold for the parametric excitation [see Fig. 4(a)]. Hence, assuming $10 \mu\text{m}$ for the active area of ∇T and $N = 1.3 \cdot 10^{-7} \text{VK}^{-1}\text{T}^{-1}$ [9] the measured voltage yields $\nabla T = 0.1 \text{mK/nm}$, which is in agreement with finite element simulations of the heat conductance for our sample geometry.

In conclusion, we have demonstrated a novel method for detecting spin waves in a thermoelectric measurement geometry by the anomalous Nernst effect. The method is based on the heat generation inside the magnetic film due to the relaxation of the spin waves to the lattice and has practically no lower limit for the wavelength of the detected spin waves. The observed effect allows for FMR and spin-wave spectroscopy in the linear and nonlinear regime with a high dynamic range and signal-to-noise ratio. It provides important insights into the generation of electromotive forces arising in ferromagnets due to magnetization dynamics, advancing the emerging field of spin caloritronics, where the interplay of magnetization dynamics, spin transport and heat transport is investigated.

The authors thank R. McMichael and M.D. Stiles for fruitful discussions and K. Suthar and S. Sankaranarayanan for finite element simulations. Work at Argonne and use of the Center for Nanoscale Materials was supported by the U.S. Department of Energy - Basic Energy Sciences under Contract No. DE-AC02-06CH11357.

-
- [1] G.E.W. Bauer, E. Saitoh, and B.J. van Wees, *Nature Materials* **11**, 391 (2012).
 - [2] A. Slachter, F.L. Bakker, J-P. Adam, and B.J. van Wees, *Nature Physics* **6**, 879 (2010).
 - [3] K. Uchida, S. Takahashi, K. Harii, J. Ieda, W. Koshibae, K. Ando, S. Maekawa, and E. Saitoh, *Nature* **455**, 778 (2008).
 - [4] C.M. Jaworski, R.C. Myers, E. Johnston-Halperin, and J.P. Heremans, *Nature* **487**, 210 (2012).
 - [5] J. Flipse, F.L. Bakker, A. Slachter, F.K. Dejene, and B.J. van Wees, *Nature Nanotechnology* **7**, 166 (2012).
 - [6] Y. Kajiwara, K. Harii, S. Takahashi, J. Ohe, K. Uchida, M. Mizuguchi, H. Umezawa, H. Kawai, K. Ando, K. Takanashi, S. Maekawa, E. Saitoh, *Nature* **464**, 262 (2010).

- [7] M.V. Costache, G. Bridoux, I. Neumann, and S.O. Valenzuela, *Nature Materials*, **11**, 199 (2011).
- [8] S.Y. Huang, W.G. Wang, S.F. Lee, J. Kwo, and C.L. Chien, *Phys. Rev. Lett.* **107**, 216604 (2011).
- [9] M. Weiler, M. Althammer, F.D. Czeschka, H. Huebl, M.S. Wagner, M. Opel, I.M. Imort, G. Reiss, A. Thomas, R. Gross, and S.T.B. Goennenwein, *Phys. Rev. Lett.* **108**, 106602 (2012).
- [10] K. Sekiguchi, K. Yamada, S.-M. Seo, K.-J. Lee, D. Chiba, K. Kobayashi, and T. Ono, *Phys. Rev. Lett.* **108**, 017203 (2012).
- [11] K. Vogt, H. Schultheiss, S.J. Hermsdoerfer, P. Pirro, A.A. Serga, and B. Hillebrands, *Appl. Phys. Lett.* **95**, 182508 (2009).
- [12] P. Pirro, T. Brächer, K. Vogt, B. Obry, H. Schultheiss, B. Leven, and B. Hillebrands, *Phys. Status Solidi B* **10**, 2404 (2011).
- [13] T. Sebastian, Y. Ohdaira, T. Kubota, P. Pirro, T. Brächer, K. Vogt, A. A. Serga, H. Naganuma, M. Oogane, Y. Ando, B. Hillebrands, *Appl. Phys. Lett.* **100**, 112402 (2012).
- [14] C. Kittel, *Phys. Rev.* **73**, 155 (1948).
- [15] F.L. Bakker, J. Flipse, A. Slachter, D. Wagenaar, and B.J. van Wees, *Phys. Rev. Lett.* **108**, 167602 (2012).
- [16] Y.S. Gui, N. Mecking, X. Zhou, G. Williams, and C.M. Hu, *Phys. Rev. Lett.* **98**, 107602 (2007).
- [17] O. Mosendz, J.E. Pearson, F.Y. Fradin, G.E.W. Bauer, S.D. Bader, and A. Hoffmann, *Phys. Rev. Lett.* **104**, 046601 (2010).
- [18] O. Mosendz, V. Vlaminck, J.E. Pearson, F.Y. Fradin, G.E.W. Bauer, S.D. Bader, and A. Hoffmann, *Phys. Rev. B* **82**, 214403 (2010).
- [19] A. Yamaguchi, K. Motoi, A. Hirohata, and H. Miyajima, *Phys. Rev. B* **79**, 224409 (2009).
- [20] M.V. Costache, S.M. Watts, C.H. van der Wal, and B.J. van Wees, *Phys. Rev. B* **78**, 064423 (2008).
- [21] Y. Yamane, K. Sasage, T. An, K. Harii, J.I. Ohe, J. Ieda, S.E. Barnes, E. Saitoh, and S. Maekawa, *Phys. Rev. Lett.* **107**, 236602 (2011).
- [22] V. Vlaminck and M. Bailleul, *Science* **322**, 410 (2008).
- [23] I. Neudecker, M. Klaui, K. Perzlmaier, D. Backes, L.J. Heyderman, C.A.F. Vaz, J.A.C. Bland, U. Rüdiger, and C.H. Back, *Phys. Rev. Lett.* **96**, 057207 (2006).
- [24] H. Schultheiss, S. Schäfer, P. Candeloro, B. Leven, B. Hillebrands, A. N. Slavin, *Phys. Rev. Lett.* **100**, 047204 (2008).
- [25] V. Vlaminck, and M. Bailleul, *Phys. Rev. B* **81**, 014425 (2010).
- [26] N. Neumann, A.A. Serga, V.I. Vasyuchka, and B. Hillebrands, *Appl. Phys. Lett.* **94**, 192502 (2009).